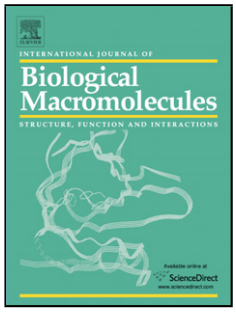

Title: An Electrochemical DNA Biosensor based on Oracet Blue as a label for detection of *Helicobacter pylori*

Author: Saeedeh hajihosseini Navid Nasirizadeh Mohammad Saeid Hejazi Parichehr Yaghmai

PII: S0141-8130(16)30317-8
DOI: http://dx.doi.org/doi:10.1016/j.ijbiomac.2016.04.009
Reference: BIOMAC 5977

To appear in: *International Journal of Biological Macromolecules*

Received date: 30-4-2015
Revised date: 25-3-2016
Accepted date: 4-4-2016

Please cite this article as: Saeedeh hajihosseini, Navid Nasirizadeh, Mohammad Saeid Hejazi, Parichehr Yaghmai, An Electrochemical DNA Biosensor based on Oracet Blue as a label for detection of Helicobacter pylori, International Journal of Biological Macromolecules http://dx.doi.org/10.1016/j.ijbiomac.2016.04.009

An Electrochemical DNA Biosensor based on Oracet Blue as a label for detection of *Helicobacter pylori*

Saeedeh hajihosseini[1], Navid Nasirizadeh[2]*, Mohammad Saeid Hejazi[3], Parichehr Yaghmai[1]

[1]Department of Biology, Science and Research Branch, Islamic Azad University, Tehran, Iran

[2]Department of Textile Engineering, Yazd Branch, Islamic Azad University, Yazd, Iran

[3]Faculty of Pharmacy, Tabriz University of Medical Sciences, Tabriz, Iran

***** Corresponding author. Tel: +98 351 8117711, Fax: +98 351 8117550

Email addresses: nasirizadeh@iauyazd.ac.ir

Abstract

An innovative method of a DNA electrochemical biosensor based on Oracet Blue (OB) as an electroactive label and gold electrode (AuE) for detection of *Helicobacter pylori*, was offered. A single–stranded DNA probe with a thiol modification was covalently immobilized on the surface of the AuE by forming an Au–S bond. Differential pulse voltammetry (DPV) was used to monitor DNA hybridization by measuring the electrochemical signals of reduction of the OB binding to double–stranded DNA (ds–DNA). Our results showed that OB–based DNA biosensor has a decent potential for detection of single–base mismatch in target DNA. Selectivity of the proposed DNA biosensor was further confirmed in the presence of non–complementary and complementary DNA strands. Under optimum conditions, the electrochemical signal had a linear relationship with the concentration of the target DNA ranging from 0.3 nmol L^{-1} to 240.0 nmol L^{-1}, and the detection limit was 0.17 nmol L^{-1}, whit a promising reproducibility and repeatability.

Keywords: DNA biosensor, Oracet Blue, Helicobacter pylori

1. Introduction

The importance of DNA in storage of the living cells information, have been using in making life of an organism by producing proteins, which have key roles in cell structure and function and run the biochemical reactions in cell [1–3]. Sequence specific working nature of the DNA, have made us to assess the functionality of the DNA and its mutation, by making different sequence detection methods for DNA, so far including Microscopy–based techniques, Mass Spectrometry, Quartz–Crystal Microbalance [4–6] Surface Plasmon Resonance (SPR) [7] and Electrochemical Biosensors [8, 9].

Electrochemical biosensors poses some advantages including but not limited to high sensitivity, easy to use, inexpensive, portable, and also need a small amounts of sample [10, 11]. The majority of the electrochemical DNA biosensors are based on DNA hybridization [8] and sequencing by hybridization is a method to be used to detect a DNA sequence [12, 13]. An electrochemical biosensor for DNA detection containing a working electrode with DNA immobilized on the surface, and the target DNA interact differently with the immobilized probe compared to the non-specific sequence [14, 15]. DNA hybridization methods mainly fall into two categories: direct and indirect protocols. Indirect strategy produces electrochemical signal during oxidation of purine base [8]. Whereas, indirect DNA hybridization is based on the utilizing of electroactive labels and monitoring its interaction with DNA strands. Some of the electroactive labels in employment in electrochemical based DNA sensing methods including hematoxylin [8], methylene blue [16–18], $[Ru(NH3)6]^{3+/2+}$[19,20], $[Fe(CN)[Co(phen)3]^{3+/2}$ ferrocene [21].

The Oracet Blue (OB) is a natural anthraquinone derivative and can be assumed as a quinine. It is proven that anthraquinone derivatives are active in electrocatalytic redox reactions of different analyses [22]. In addition, the application of the OB in

electrochemical sensors have been confirmed before, by using for detection of hydroxylamine [22] and simultaneous determination of dopamine, ascorbic acid and uric acid [23].

H. pylori could promote serious health problems of the stomach and could cause cancer probably due to the enhanced production of free radicals near *H. pylori* and an increased rate of host cell mutation and/or through the "perigenetic pathway", by means of alterations in the cell proteins, such as adhesion proteins [24–26]. Detection of the *H. pylori* could help us to enhance the quality of the life and also to prevent more serious health problems such as cancer [24–26].

Herein, a new electrochemical biosensor is introduced based on interaction of OB with a 18–mer deoxyoligonucleotide chain of *cag* gene of *H. pylori* for detection of this bacterium based on DNA hybridization using the self–assembled monolayer (SAM) technique.

2. Materials and Methods

2.1. Materials

All the chemicals used here without further purification. 6–Mercapto–1–hexanol (MCH) was supplied from Aldrich, whereas the OB and the rest of chemical reagents were purchased from Merck Company. All the solutions were prepared with double distilled (DI) water. Oligonucleotides were supplied (as lyophilized powder) from Eurofins MWG Operon with the following sequences: Thiolated DNA probe (H. pylori): 5'–HS $(CH_2)_6$ AGA CAT GCA AAA AGG TAT –3'. Complementary target DNA (H. pylori): 5'– AGA CAT GCA AAA AGG TAT –3'. Non–complementary DNA: 5'–GAA TAT GAT TTA CAG TTT ATT TTT–3'. Mis-Match DNA (H. pylori):

5'– AGA CAT GCT AAA AGG TAT –3'. The stock solutions of the oligonucleotides (100.0 µmol L^{-1}) were prepared with 10 mmol L^{-1} Tris–HCl buffer (pH 8.0) containing 1.0 mmol L^{-1} of EDTA, and were kept frozen at –20 °C. The immobilization and hybridization solutions were 1.0 mol L^{-1} phosphate buffer (pH 4.5) and 0.05 mol L^{-1} phosphate buffer (pH 7.0) containing 0.3 mol L^{-1} of NaCl, respectively. The washing solution was also 0.05 mol L^{-1} phosphate buffer (pH 7.0) containing 0.3 mol L^{-1} of NaCl. A stock solution of 1.0 mmol L^{-1} of OB was prepared by dissolving the OB powder in methanol and afterwards addition of the 0.1 mol L^{-1} phosphate buffer solution with pH 7.0

2.2. Instrumentations

An Autolab potentiostat/galvanostat model PGSTAT 30 (Eco. Chemic, Utrecht, Netherlands) were used to accomplish all the electrochemical measurements. The potentiostat/galvanostat was connected to the conventional three–electrode system includes Gold electrode (AuE) (with surface area of 0.0314 cm^2) as the working electrode, a saturated calomel electrode (SCE) as the reference electrode, and a platinum electrode as the auxiliary electrode. All the potential in the text were reported with respect to this reference electrode. The GPES software on a regular computer were used as an interface of the electrochemical system.

2.3. Preparation of probe–modified electrode and DNA hybridization

First, surface of the AuE was polished with a 1.0 µm and 0.05 µm alumina–water slurry on a smooth polishing fabric, and it was rinsed with DI water and dried under nitrogen stream. Then, 2.5 µL droplet of immobilization buffer solution containing 9.0

µmol L^{-1} *H. pylori* probe (ss–DNA) was deposited on the AuE surface for the probe self–assembly and the electrode were incubated at room temperature (25±1 °C) for 105 min in a high–humidity container. Consequently, *H. pylori* self–assembled electrode (ss–DNA/AuE) was washed with the washing solution and incubated in 1.0 mmol L^{-1} solution of MCH for 5 min. Then, the electrode was rinsed with 80:20 (v/v) ethanol: water and distilled water, respectively. The hybridization was performed by immersing the ss–DNA/AuE into the hybridization buffer solution (pH 7.0) containing desired concentration of the target oligonucleotide (complementary, mismatch or non-complementary strands) at room temperature (25±1 °C) for 120 min resulting in hybridization of the sample DNA with the probe and generating dsDNA/AuE.

OB was accumulated on the dsDNA/AuE by immersing the modified electrode into 0.1 mol L^{-1} phosphate buffer solution (pH 7.0) containing 0.09 mmol L^{-1} of OB without applying any potential to the electrode, while gently stirred at 100 rpm for 90.0 min. Afterward, the accumulated electrode was rinsed with washing solution for 10 s. A similar procedure was applied to the accumulation of OB on a bare AuE electrode.

The electrochemical measurements were performed using (DPV), with an amplitude of 25 mV, at modulation time of 0.05 s, and a step potential of 50 mV in 0.1 mol L^{-1} phosphate buffer solution (pH 7.0). The raw data were processed with the Savitzky and Golay filter (level 2) of the GPES software, followed by the GPES software moving average baseline correction using a 'peak width' of 0.01.

In addition, in order to assess every modification of the biosensor preparation, the cyclic voltammetry (CV) and electrochemical impedance spectroscopy (EIS) were performed in $K_3[Fe(CN)_6]$ solution, for the modified electrode. The CV was performed in 1.0 mmol L^{-1} $K_3[Fe(CN)_6]$ in PBS buffer at the potential range of -0.025 to 0.33 V and a sweep rate of 0.02 V s^{-1}; and the EIS was performed in a solution of 5.0 mmol L^{-}

[1] $K_3[Fe(CN)_6]$/ $K_4[Fe(CN)_6]$ containing 1.0 mol L^{-1} KCl, from 100 kHz to 0.01 Hz with amplitude 5 mV and potential 0.27 V. Moreover, to assess the selectivity, after preparation of the biosensor, it was incubated in the hybridization solution with the mis-match and non-complementary sequences, with the same circumstances of the hybridization and DPV voltammograms were recorded. As a final point, the scheme 1 is representing a brief overview of the biosensor preparation steps and working mechanism.

Scheme 1

3. Results and discussion

3.1. Self–assembly of the ss–DNA on AuE

The ss–DNA was immobilized using two different methods, droplet and solution method. In droplet self–assembly, a 2.5 µL droplet of *H. pylori* probe solution was putted onto the bare AuE. On the other hand, in the solution method, the bare AuE was immersed in the immobilization buffer containing 9.0 µmol L^{-1} probe solution for 105 min. Afterwards, the both prepared electrodes were soaked first in the MCH and subsequently in the OB solution. Similarly, OB was accumulated on ds–DNA modified electrode, so that probe self–assembled AuE was immersed in the target DNA solution and then in the OB solution. Fig. 1A illustrates the differential pulse voltammograms (DPVs) of the accumulated OB on the surface of ss–DNA/AuE before (curves a and b) and after hybridization with the complementary DNA (curves c and d) using the prepared electrodes by the droplet (curves b and d) and the solution self–assembly (curves a and c).

(Figure 1)

As illustrated, the current respond of the OB accumulated on ssDNA/AuE prepared by the droplet method (curve b) is higher than the one obtained from the solution method (curve a). Besides, the results demonstrate that after the hybridization process, the current respond obtained from the first method (curve d) is larger than that taken from the solution method (curve c), suggesting that the probe molecules are better self–assembled in the droplet method. The fabrication steps of the ss–DNA/AuE and ds–DNA/AuE as well as their interaction with OB label was shown in scheme 1.

Fig. 1B demonstrations the current response of accumulated OB on ss–DNA/AuE versus required time for the probe self–assembly. The results showed that the accumulated OB current response enhances with increasing the probe immobilization time up to about 105 min and slightly decreased after 105 min. This may be due to the gold electrode surface which is thoroughly covered by the DNA probe after 105 min. Therefore, the time of 105 min was, chosen for probe immobilization in subsequent experiments.

Fig. 1C shows the results of DPV measurements related to the OB accumulated on ss–DNA/AuE versus the concentration of the probe. As it cab be seen, the current response of accumulated OB increased to about 9.0 µmol L^{-1} and then slightly decreased with the increase of the probe concentration. This is in agreement with findings of Nasirizadeh and his coworkers [8], massive accumulation of the probe on the electrode result in less availability of OB to DNA.

As shown, similar trend is observed in both experiments of probe concentration and self–assembly time, whereupon can be explained that electrode surface have distinct capacity for accumulation of DNA probe. Based on obtained results, 9.0 µmol L^{-1} of

thiolated DNA was selected as an optimum concentration for the immobilization of the ss–DNA on the bare AuE.

3–2. Optimization of the hybridization process

Three different methods were employed for DNA hybridization and their results compared together. In the first method, which is named droplet method, the hybridization process was conducted by depositing 2.5 µL droplet of the complementary solution onto the ss–DNA/AuE, for prevent evaporation, it incubated in a high–humidity container at room temperature (25±1 °C) for 2.0 h. Finally, the modified electrode was rinsed thoroughly in a washing solution with 100 rpm stirring, and then OB was accumulated on the modified electrode surface. The DPV diagram accumulated OB on this electrode surface is shown in Fig. 2 curve a. In the second, called preheated solution hybridization method, the ss–DNA/AuE was soaked in the hybridization solution at 85 °C for 3 min when the solution was moderate stirred. Then, the solution was cooled down gradually at room temperature. Thereafter, the electrode was rinsed with a washing solution and OB was accumulated on the electrode. Fig. 2 curve b, presents the DPV of the accumulated OB by the preheated solution hybridization method. Last method, solution hybridization method (protocol), which was done by similar described method in section 2.3. After hybridization, the modified electrode was immersed in the OB solution. Fig. 2 curve c, illustrated the current peak of modified electrode by solution method. As indicated, the highest current response was observed in the modified electrode with solution method.

It could express that in solution protocol, target DNA have good chance for gain the best orientation for the hybridization. According to Fig. 2 the solution hybridization method was suggested as an optimal procedure for the hybridization process.

(Figure 2)

3–3. Optimization of OB accumulation on the modified electrode surface with ds–DNA

To discover the best concentration of OB as an electroactive label on modified electrode with the ds–DNA. Thus, after hybridization process, modified gold electrode was immersed in different concentrations of OB for 90 min. The accumulated OB DPVs after immersing ds–DNA/SAM in different concentrations of the OB is shown in Fig. 3A. As it is presented, the signals of accumulated OB enhanced with the increase of OB concentration (Fig. 3B). The highest cathodic current was observed at the concentration of 0.9 mmol L^{-1} of OB and then remained relatively constant which is considered as the optimal concentration of OB. In addition, the effect of accumulation time of OB was also investigated. Based on the results given in Fig. 3C, the best time for accumulation OB on ds–DNA/SAM was 90 min.

(Figure 3)

3–4 Analytical performance and selectivity of the DNA biosensor

The selectivity of the DNA hybridization on the Au electrode with probe DNA was evaluated by hybridizing with its complete complementary sequence, mismatch sequence, and non-complementary sequence. Fig. 4 shows the DPVs of OB accumulated on the MCH modified AuE (curve a), ss–DNA/AuE before (curve b) and after hybridization with 2.0 µmol L^{-1} solution of non–complementary (curve c), mismatch (curve d) and complementary (curve e) oligonucleotides.

As shown in Fig. 4 as compared with the DPV response of OB with ss–DNA modified AuE (curve b), probe DNA a pronounced increase in the peak current value of the OB was observed when hybridized with its complementary sequence (curve e).

The current peak obtained by probe hybridization with mismatch DNA (curve d) was higher than one with non–complementary sequence (curve c). The results showed that the modified electrode had satisfactory selectivity for DNA hybridization.

(Figure 4)

In addition to the DPV analysis, the CV and EIS analysis were also done to confirm the selectivity of the biosensors and also to confirm every modification steps of the electrode. In the Fig 5A, the resulted cyclic voltammograms of the modified electrode in the 1.0 mmol L^{-1} $K_3[Fe(CN)_6]$ solution after every modification, are shown. As it can be seen in this Fig, the bare AuE (curve a) has a high current voltammogram, and after ss-DNA immobilization on the AuE, the current decreases vividly due to the blocking of the $[Fe(CN)_6]^{3-/4-}$ anions to reach the AuE surface (curve b), while the MCH treatment of the ss–DNA/AuE increases the current of the voltammogram, which could be because of removing incorrectly orientated ss-DNA (curve c). Hybridization of the target DNA with the ss-DNA on the AuE is also cause a large decrement in current (curve e), but the mismatched target DNA have higher current due to its incomplete hybridization to the ss-DNA on the AuE.

The Fig 5 B, is representing the Nyquist plot of the different electrodes in the solution of 5.0 mmol L^{-1} $K_3[Fe(CN)_6]$/ $K_4[Fe(CN)_6]$ containing 1.0 mol L^{-1} KCl. The curve (a) is corresponding to the Bare AuE which have a very low resistance. When the ss-DNA is immobilizing on the AuE, the charge transfer resistance (R_{ct}) of the electrode is

increasing due to the blockage of the $[Fe(CN)_6]^{3-/4-}$ into the AuE surface (curve b), but after MCH treatment the R_{ct} is decreasing a little (curve c).

The target hybridized/probe modified AuE showed a significantly higher charge transfer resistance (curve e), but the mismatched target is having a very lower R_{ct} (curve d), which could be because of incomplete hybridization of the mismatched DNA compared to the complementary target DNA. The observations of the above-mentioned CV and EIS studies are in support of each other, and also confirming the electrode modification steps to form the proposed biosensor and the good selectivity of the biosensor.

(Figure 5)

Fig. 6A displayed the DPV hybridization responses for increasing target concentrations of complementary sequence from 0.30 nmol L^{-1} to 240.0 nmol L^{-1}. The peak currents of intercalated OB was increased with the increment of the complementary target DNA concentrations and were linear with the value of the complementary target DNA concentrations, as shown in the inset of Fig. 6B. The linear regression equation was y=–0.6021x–94.105 with a correlation coefficient value of 0.998 (x is the concentration of complementary sequence, the peak current of OB, nA).

The calibration plot, in the range of 0.3–240.0 nmol L^{-1} of DNA target, was used to estimate the lower limit of DNA target detection at ss–DNA/AuE. According to the method mentioned in the references [27], the lower detection limit, Cm, was obtained to be 0.17 nmol L^{-1} by using the equation $Cm = 3s_{bl}/m$, where s_{bl} is the standard deviation of the blank response (nA) and m is the slope of the calibration plot (–0.6021 nA nmol L^{-1}). The average voltammetric current and the precision estimated in terms of relative

standard deviation (CV) for ten repeated measurements (n=12) of 40.0 nmol L^{-1} of the target DNA were 121.0 ± 4.3 nA and 3.6% respectively.

In addition, the repeatability of the biosensor was assured by low relative standard deviation (RSD) of all the measurements, which were ranging from 3.1 to 4.5 %, for different concentrations of the target DNA. Moreover, the reproducibility of the biosensor was guaranteed by making the biosensor for several times (5 times) and testing in a similar condition and concentration, and comparing the results. The RSD of the 5 times preparation of the biosensor was 4.2 %, which is very low and representing the high reproducibility of the biosensor.

Table 1, representing the comparison of the biosensor analytical characteristics with those previously reported by others [8, 28-35]. As it can be seen, the specifications of the biosensor are superior in some cases, especially linear range and detection limit, to those of the previously reported.

(Figure 6)

(Table 1)

4. Conclusions

In this study, the interaction of OB as an electroactive DNA label was investigated. The different affinity of OB to ss–DNA and to ds–DNA is employed for the development of a DNA biosensor for the detection and discrimination of *H. pylori* corresponding to oligonucleotide from non–complementary DNA. The experiments also confirm that OB–based DNA biosensor have capability of detection the single–base mismatch in target DNA. This study indicates the best method for probe self–assembly is drop self–assembly and also found the solution hybridization as the best hybridization method. Under optimum conditions, the electrical signal has a linear

relationship with the concentration of target DNA ranging from.3 nmol L^{-1} to 240.0 nmol L^{-1}, and the detection limit is 0.17 nmol L^{-1}.

5. References

[1] T.A. Hall, B. Budowle, Y. Jiang, L. Blyn, M. Eshoo, K.A. Sannes–Lowery, R. Sampath, J.J. Drader, J.C. Hannis, P. Harrell, V. Samant, N. White, D.J. Ecker, S.A. Hofstadler, Anal. Biochem. 344 (2005) 53–69.

[2] H. Ilkhani, M. Ganjali, M. Arvand, M. Hejazi, F. Azimi, P. Norouzi, Int. J. Biol. Macromol. 49 (2011) 1117–1123.

[3] N. Stellwagen, C. Gelfi, P.G. Righetti, Electrophoresis. 23 (2002) 167–175.

[4] N. Tretyakova, W.P. Villalta, S. Kotapati, Chem. Rev. 113 (2013) 2395–2436.

[5] C.M. Dixon, J. Biomol. Tech. 19 (2008) 151–158.

[6] J.R. Edwards, H. Ruparel, J. Ju, Mutat. Res. 573 (2005) 3–12.

[7] M.L. Ermini, S. Mariani, S. Scarano, M. Minunni, Biosens. Bioelectron. 40 (2013) 193–199.

[8] N. Nasirizadeh, H.R. Zare, M.H. Pournaghi–Azar, M.S. Hejazi, Biosens. Bioelectron. 26 (2011) 2638–2644.

[9] C. Zhang, J. Lou, W. Tu, J. Bao, Z. Dai, Analyst 140 (2015) 506–511.

[10] Y. Hu , X. Xu, Q. Liu, L. Wang, Z. Lin, G. Chen, Anal. Chem. 86 (2014) 8785–8790.

[11] E. Hamidi–Asl, J.B. Raoof, R. Ojani, S.M. Golabi, M. S. Hejazi, J. Iran. Chem. Soc. 10 (2013) 1075–1083.

[12] H. Jin, M. Wei, J. Wang, Chem. Cent. J. 7 (2013) 65.

[13] M.S. Hejazi, E. Alipour, M.H. Pournaghi–Azar, Talanta 71 (2007) 1734–1740.

[14] J.B. Raoof, R. Ojani, S.M. Golabi, E. Hamidi–Asl, M.S. Hejazi, Sensor. Actuat B Chem. 157 (2011), 195–201.

[15] B. Zhu, M.A. Booth, P. Shepherd, A. Sheppard, J. Travas–Sejdic, Biosens. Bioelectron. 15 (2015) 74–80.

[16] A. Erdem, K. Kerman, B. Meric, D.S. Ozkan, P. Kara, Turk. J. Chem. 26 (2002) 851–862.

[17] H .Xu, S. Gao, F. Hou, Curr. Phys. Chem. 1 (2011) 7–10.

[18] Y. Jin, X. Yao, Q. Liu, J. Li, Biosens. Bioelectron. 22 (2007) 1126–1130.

[19] S.W. Dutse, N.A. Yusof, H. Ahmad, M.Z. Hussein, Z. Zainal, Int. J. Electrochem. Sci. 7 (2012) 8105–8115.

[20] Q. Wang, Y. Ding, F. Gao, S. Jiang, B. Zhang, J. Ni, F. Gao, Anal. Chim. Acta. 788 (2013) 158–164.

[21] X. Luo, T. Ming–Hung, L. Ming Hing, Anal. Chem. 80 (2008) 7341–7346.

[22] H.R. Zare, N. Nasirizadeh, J. Braz. Chem. Soc. 23 (2012) 1070–1077.

[23] H.R. Zare, N. Rajabzadeh, N. Nasirizadeh, M. M. Ardakani, J. Electroanal. Chem. 589, (2006) 60-69.

[24] J.C. Atherton, Annul. Rev. Pathol. 1 (2006) 63–96.

[25] J.G. Kusters, A.H. Van Vliet, E.J. Kuipers, Clin. Microbiol. Rev. 19 (2006) 449–490.

[26] J. Parsonnet, G.D. Friedman, D.P. Vandersteen, Y. Chang, J.H. Vogelman, N. Orentreich, R.K .Sibley. N. Engl. J. Med. 325 (1991) 1127–1131.

[27] D.A. Skoog, F.J. Holler, T.A. Nieman, 1998. Principles of Instrumental Analysis, 5th ed. Harcourt Brace, Philadelphia.

[28] E. Souza1, G. Nascimento, N. Santana, D. Ferreira, J. Bibiano, M. Arruda, D. Bruneska, J. Filho. Biosens. J. 3(2014) 107.

[29] N. Mansor, Z. Mohd Zain, H. Hamzah, M .Noorden, S. Jaapar, V. Beni, Z. Ibupoto. Open Journal of Applied Biosensor 3(2014) 9-17.

[30] L. Zhu, R. Zhao, K. Wang, H. Xiang , Z. Shang ,W. Sun. Sensors. 8(2008) 5649-5660.

[31] G.A. Nascimento, E. Souza, D. erreira, M.S. Arruda,C. Castelletti, M. Wanderley, M. Ekert, D. Bruneska, J. Filho. Biosens. Bioelectron. 38 (2012) 61–66.

[32] S. Jampasa, W. Wonsawat, N. Rodthongkum, W. Siangproh, P. Yanatatsaneejit, T Vilaivanf, O. Chailapakul, Biosens. Bioelectron. 54 (2014) 428–34

[33] D.S. Campos-Ferreira , G.A. Nascimento, E.V. Souza, M.A. Souto-Maior, M.S. Arruda, D.M. Zanforlin, D. Bruneska, J.L. Lima-Filho, Anal. Chim. Acta. 804 (2013) 258-263.

[34] H. Huang, W. Bai, C. Dong, R. Guo , Z. Liu. Biosens. Bioelectron. 68 (2015) 442–446

[35] Z. Shakoori, S. Salimian, S. Kharrazi, M. Adabi, R .Saber. Anal. Bioanal. Chem. 407 (2014) 455-461.

Table 1 Comparison of the analytical parameters of different biosensors for DNA determination.

Electroactive indicator	Linear range / nmol L^{-1}	Detection limit / nmol L^{-1}	Electrochemical method	Mismatch detection	Electrode	References
Hematoxylin	12.5-350.0	3.8	DPV	Single-base mismatch	gold electrode	8
Methylene Blue	2-10	1.49	DPV	– –	pencil graphite	28
ZnO Nanowires	1×10^{4}-1×10^{5}	3.32×10^{3}	DPV	– –	gold electrode	29
Methylene Blue	50-1×10^{5}	36.0	CV	– –	gold electrode	30
Methylene Blue	5-100	4.35	DPV	– –	gold electrode	31
Anthraquinone	20.0- 12000	14	DPV	– –	screen-printed carbon electrode	32
Methylene Blue	18.75-250	18.13	DPV	– –	gold electrode	33
$[Ru(phen)_3]^{2+}$	0.0001 - 0.1	4×10^{-5}	DPV	–	glassy carbon electrode	34
$[Co(phen)_3]^{3+}$	0.001 - 1.0×10^{3}	2×10^{-4}	CV	Single-base mismatch	gold electrode	35
OB	0.3–360	0.17	DPV	Single-base mismatch	gold electrode	This work

Figure captions:

Fig. 1. (A) DPVs of the OB accumulated on the surface of ss–DNA/AuE before (voltammograms of a and b) and after hybridization with the complementary DNA (voltammograms of c and d) using the electrodes prepared with two different methods of the droplet self–assembly (voltammograms of b and d) and the solution self-assembly (voltammograms of a and c). The accumulated OB current response on ss–DNA/AuE versus (B) the consumed time for the probe self–assembly, (C) the probe concentration.

Fig. 2. DPVs of the OB accumulated on the surface of ds–DNA/SAM that were prepared with different hybridization methods of (a) the drop hybridization, (b) the preheated solution hybridization and (c) the solution hybridization.

Fig. 3. (A) DPVs of the OB accumulated on the surface of ds–DNA/SAM that were prepared with different OB concentration. The letters (a) to (i) correspond to 0.015– 0.135 mmol L^{-1} OB. (B) The accumulated OB current response on ds–DNA/AuE versus the different OB concentration. (C) The consumed time for the OB accumulated.

Fig. 4. DPVs of the OB accumulated on the (a) MCH modified AuE, ss– DNA/AuE before (b) and after hybridization with 2 µmol L^{-1} oligonucleotide solution of the (c) non–complementary, (d) mismatch, and (e) complementary in 0.1 mol L^{-1} phosphate buffer solution (pH 7.0).

Fig 5. (A) The CVs of the modified electrode in the 1.0 mmol L^{-1} $K_3[Fe(CN)_6]$ solution after every modification step of the electrode. (a) bare AuE, (b) ss–DNA/AuE, (c) MCH/ss–DNA/AuE, (d) mismatched target DNA, and (e) Target DNA. **(B)** The Nyquist plot of the different electrodes in the solution of 5.0 mmol L^{-1} $K_3[Fe(CN)_6]/K_4[Fe(CN)_6]$ containing 1.0 mol L^{-1} KCl. (a) Bare AuE, (b) ss–DNA/AuE, (c) MCH/ss–DNA/AuE, (d) mismatched target DNA, and (e) Target DNA.

Fig. 6. (A) DPVs of the OB accumulated on the hybridized ss–DNA/AuE with different concentrations of the complementary (target) DNA in 0.1 mol L^{-1} phosphate buffer solution (pH 7.0). The numbers of 1–12 correspond to 0.3–360.0 nmol L^{-1} target DNA.(B) Inset shows the plot of difference in the accumulated OB current response on ds–DNA/AuE and ss–DNA/SAM ($\Delta I = I_{ds-DNA} - I_{ss-DNA}$) versus the target DNA concentration in hybridization process.

Scheme. 1

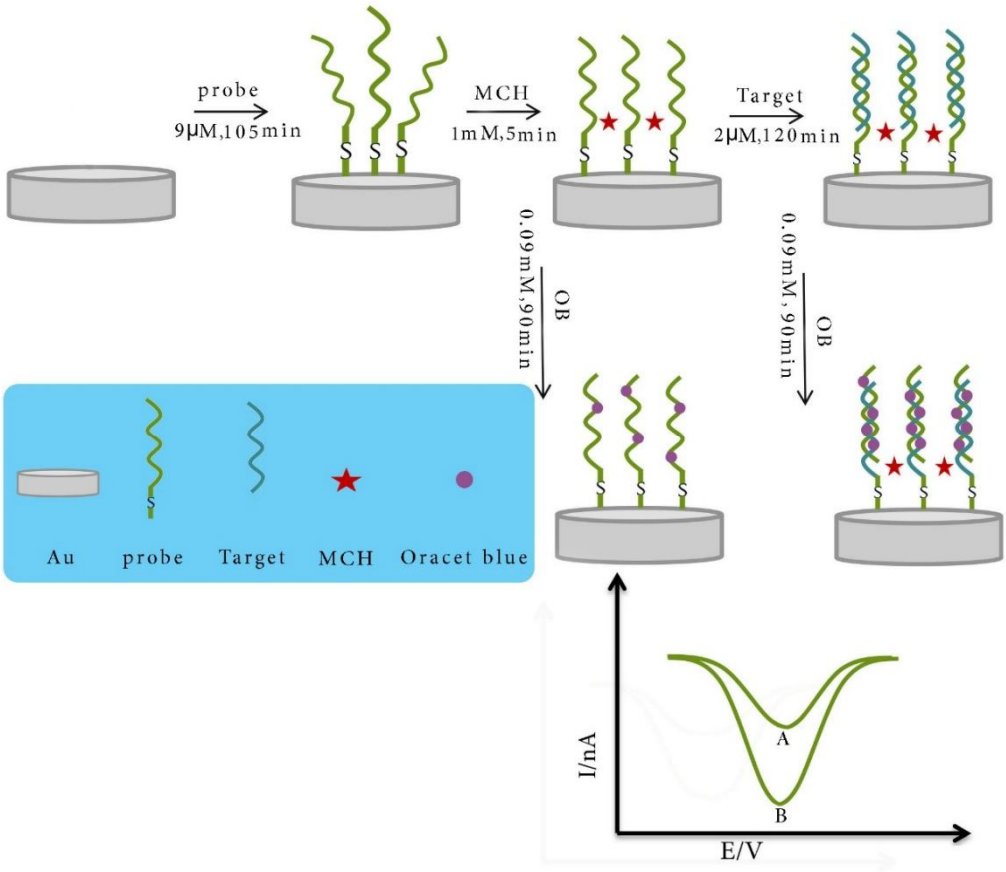

Fig. 1

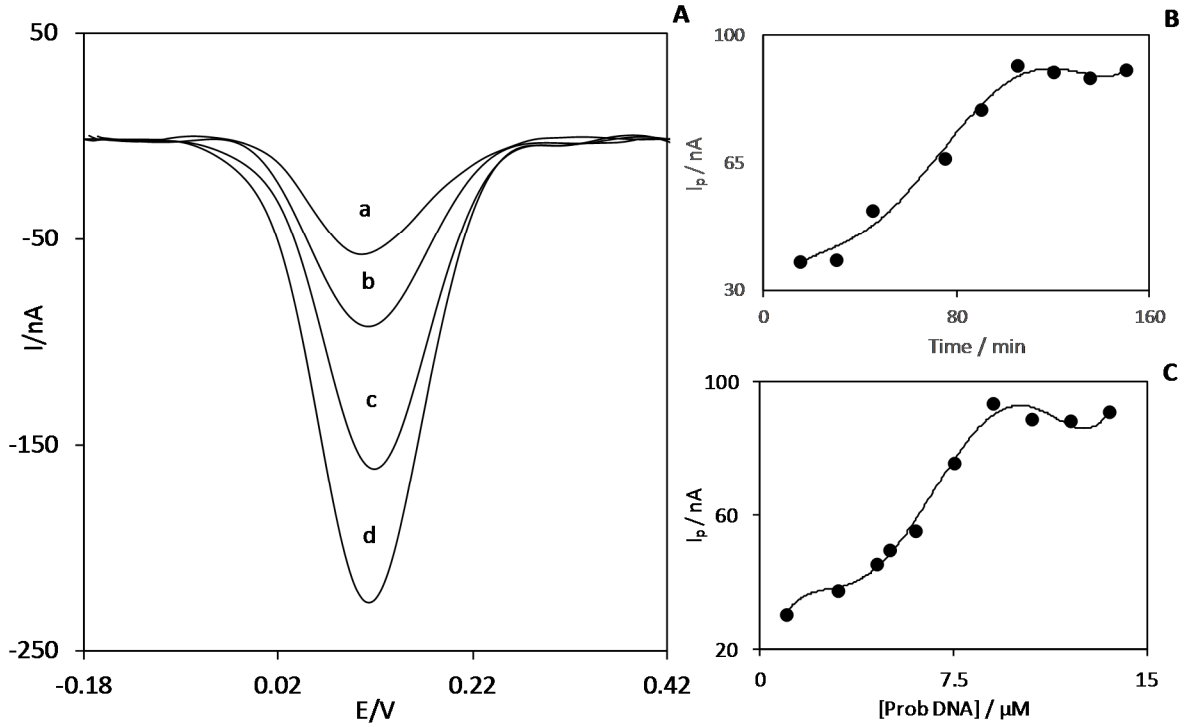

Fig. 2

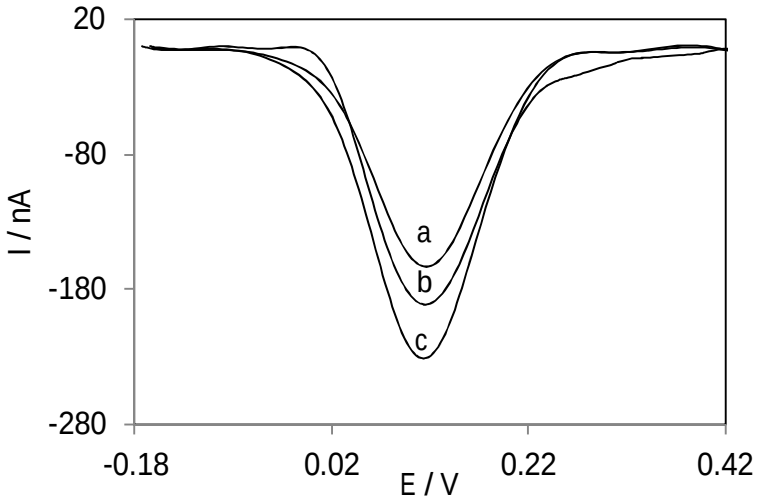

Fig. 3.

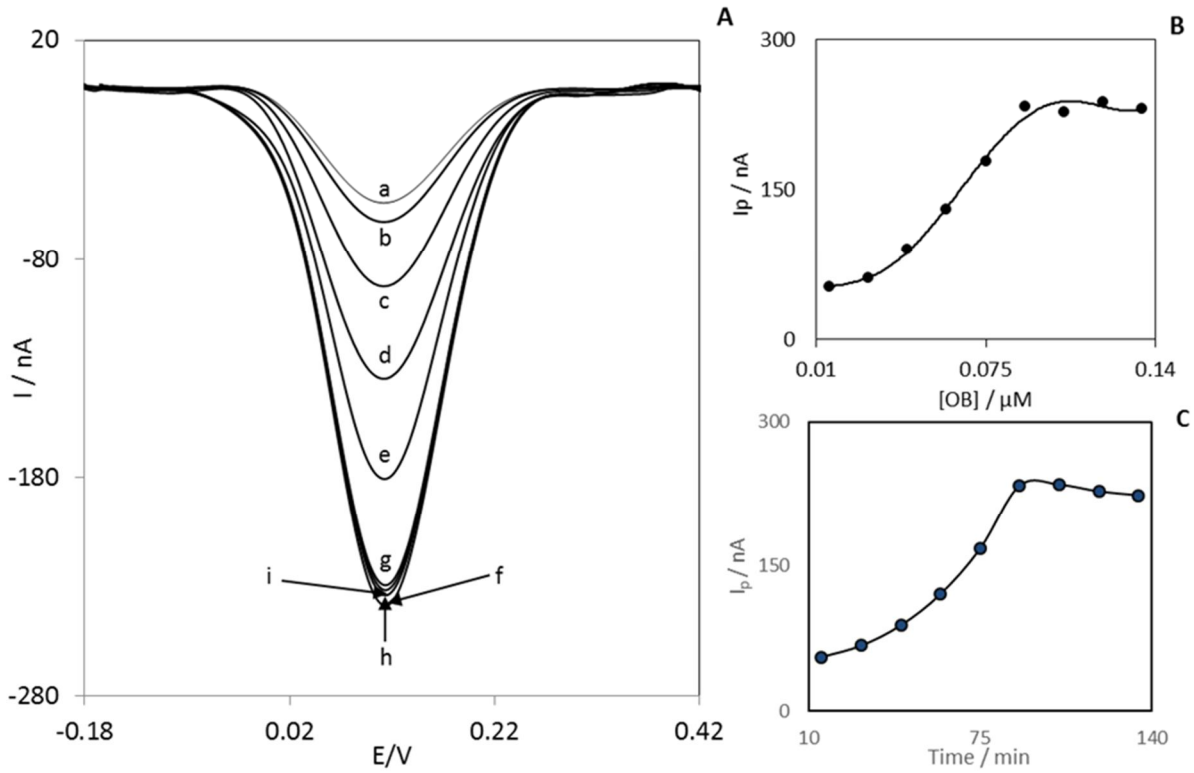

Fig. 4.

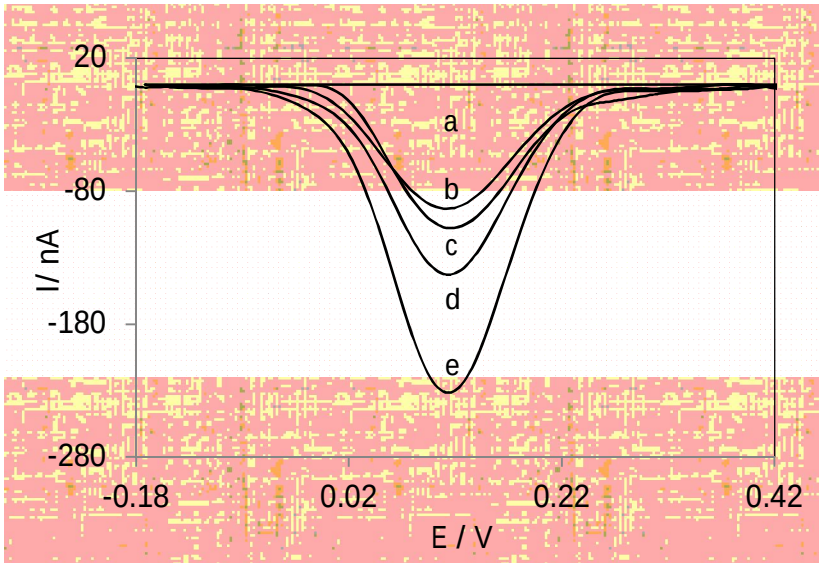

Fig 5.

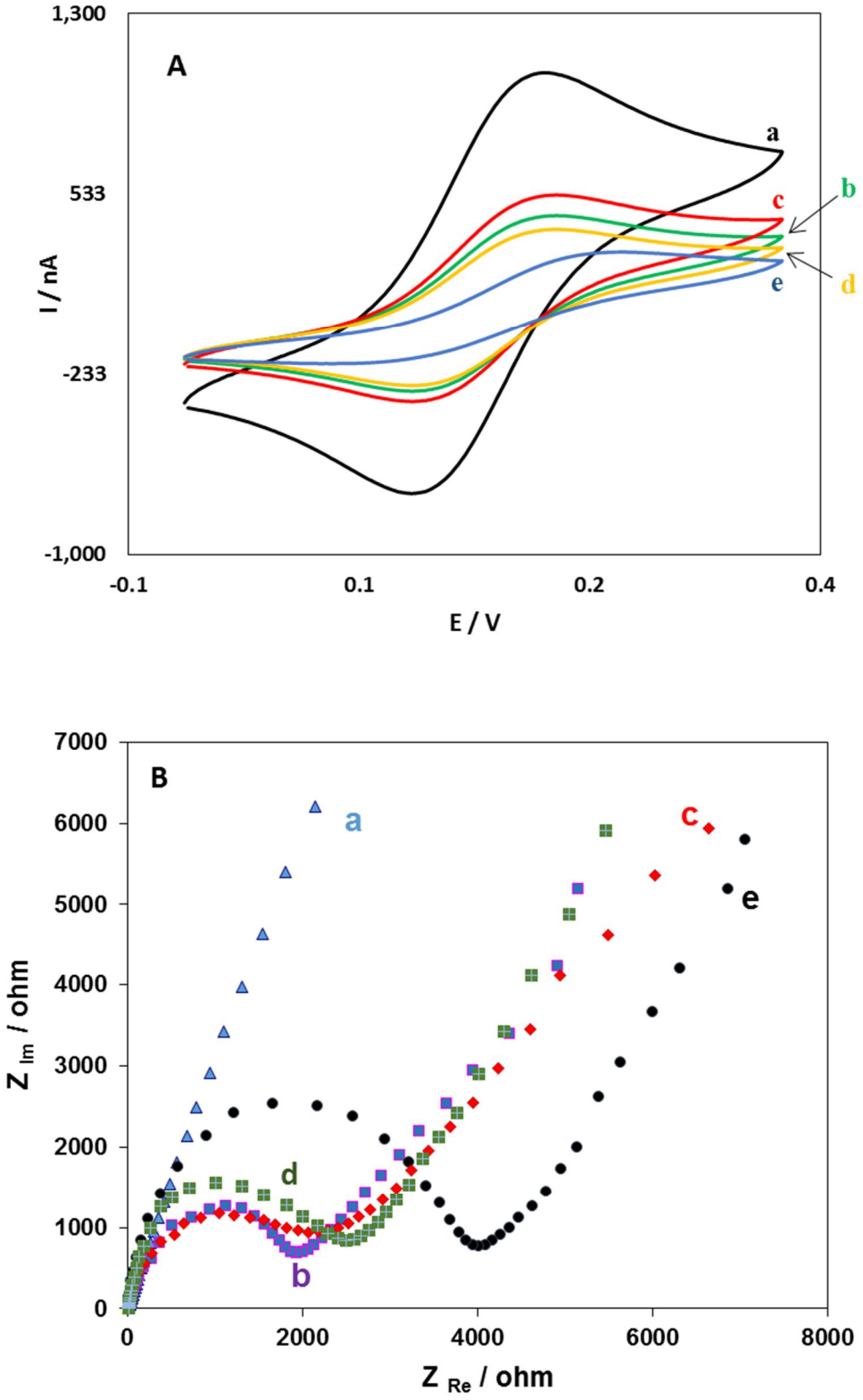

Fig. 6.